European Journal of Radiology Open 14 (2025) 100662

Contents lists available at ScienceDirect

European Journal of Radiology Open

journal homepage: www.elsevier.com/locate/ejro

The role of resting-state perfusion CMR in the evaluation of microvascular obstruction in patients with acute myocardial infarction: A clinical perspective

Yingying Hu [a,b,1], Zidi Wang [a,c,1], Zheng Sun [a,*], Zhi Liu [d], Jie Lu [a,*]

[a] Department of Radiology and Nuclear Medicine, Xuanwu Hospital, Capital Medical University, Beijing 100053, PR China
[b] Department of Radiology, Peking University International Hospital, Beijing 102206, PR China
[c] Yangjing Medical college, Capital Medical University, Beijing 101300, PR China
[d] Department of Emergency, Xuanwu Hospital, Capital Medical University, Beijing 100053, PR China

ARTICLE INFO

Keywords:
Cardiac magnetic resonance
Resting-state perfusion weight imaging
Acute myocardial infarction
Microvascular obstruction

ABSTRACT

Objectives: To investigate the clinical application value of cardiac resting-state perfusion weight imaging (rs-PWI)-derived parameters in patients with acute myocardial infarction (AMI) complicated by microvascular obstruction (MVO).

Methods: Overall, 300 patients with AMI were prospectively enrolled, and divided into the MVO and non-MVO groups, based on the presence of MVO in the infarcted myocardium. Differences in rs-PWI imaging parameters, and the diagnostic value of rs-PWI in reperfusion myocardial ischemia at segment level and MVO were quantitatively evaluated.

Results: The average age was 58.60 ± 13.03 years, and 246/300 (82 %) were males. The MVO group had 176 patients (mean age: 57.90 ± 12.47), including 140 (80 %) males. The left ventricular (LV) volumes occupied by the infarcted myocardium were 19.60 ± 2.70 %LV and 15.20 ± 3.40 %LV in the MVO and non-MVO groups, respectively ($P < 0.05$). There were 679 LGE positive segments in the MVO group (679/2816, 24.1 %). The area under curve (AUC), sensitivity, specificity, and Jordan index of rs-PWI for MVO diagnosis were 0.95(0.89–0.99), 94.3 %, 93.4 %, and 0.88, respectively. At the segmental level, the maximum rising slope was higher in the MVO than non-MVO group (15.09 ± 2.64 vs. 6.21 ± 1.25, $P < 0.05$). The time to peak 20 %-80 % was shorter in the MVO group (4.07 ± 0.79 vs. 7.75 ± 1.03, $P < 0.05$). Comparison revealed differences in perfusion indices (MVO: 0.32 ± 0.09 vs. non-MVO: 0.42 ± 0.04, $P < 0.05$). The highest diagnostic value for MVO among rs-PWI parameters was AUC 0.90(0.84–0.97), sensitivity 94.1 %, specificity 88.7 %, and accuracy 91.1 %.

Conclusion: CMR rs-PWI sequence effectively evaluates reperfusion myocardial ischemia complicated with MVO, while the perfusion index has high diagnostic value in quantifying myocardial blood flow potential.

Abbreviations: AHA, American Heart Association; AMI, Acute Myocardial infarction; BNP, B-type natriuretic peptide; CE-SSFP, Contrast-enhanced SSFP; CK-MB, Creatine kinase isoenzyme; CMR, Cardiac magnetic resonance; D2B, Door to balloon; DSA, Digital subtraction angiography; EDV, end-diastolic volume; EGE, Early gadolinium enhancement; ESV, end-systolic volume; LAD, Left anterior descending artery; LCX, Left circumflex artery; LGE, Late gadolinium enhancement; LV, Left ventricular; LVEF, left ventricular ejection fraction; MPF, Myocardial perfusion fraction; MVO, Microvascular obstruction; PCI, Percutaneous coronary intervention; RCA, Right coronary artery; ROI, Region of interest; Rs-PWI, resting state-perfusion weight imaging; SD, Standard deviation; TIMI, Thrombolysis in myocardial infarction; TNI, Troponin.

* Correspondence to: Department of Radiology and Nuclear Medicine, Xuanwu Hospital, Capital Medical University, No. 45 of Changchun Street, Xicheng District, Beijing 100053, PR China.

E-mail addresses: yingyinghu_0105@163.com (Y. Hu), wzd996990@gmail.com (Z. Wang), sunzheng@xwhosp.org (Z. Sun), liuzhi@xwhosp.org (Z. Liu), imaginglu@hotmail.com (J. Lu).

[1] These authors contributed equally to this work and share the first authorship.

https://doi.org/10.1016/j.ejro.2025.100662
Received 18 March 2025; Received in revised form 13 May 2025; Accepted 22 May 2025

1. Introduction

Most patients with acute myocardial infarction (AMI) treated with primary percutaneous coronary intervention (PCI) ultimately achieve complete restoration of the epicardial blood flow in the infarct-related artery [1,2]. Despite adequate angiographic results, myocardial perfusion remains impaired in many patients, and outcomes can vary [3]. Insufficient perfusion of the microvasculature can lead to higher rates of post-infarction complications and adverse left ventricular remodeling [3,4]. Hence, preservation of the microvasculature plays a critical role in AMI patients treated with primary PCI [5], because normal myocardial tissue shows normal first-pass perfusion after injection of the contrast agent, whereas coronary artery stenosis or obstruction can lead to local microcirculatory dysfunction, with a reduced signal from the diseased myocardium during first-pass perfusion, when little or no contrast agent enters the infarcted myocardium [6]. However, data regarding the correlation between microvascular perfusion and cardiac magnetic resonance (CMR) outcomes remains limited.

CMR imaging is a widely applied noninvasive and non-radiation imaging method that can achieve excellent soft tissue resolution, high temporal and spatial resolution and arbitrary plane imaging [7]. This technique allows the comprehensive evaluation of cardiac shape, ventricular function, myocardial perfusion, and tissue characteristics, as well as the quantification of blood flow; as such, it is considered the gold standard for evaluating cardiac function and for noninvasive myocardial tissue analysis [8]. As technology has advanced, CMR myocardial perfusion imaging has been able to quantitatively evaluate myocardial microvascular, accurately detect ischemic myocardial disease, and evaluate myocardial viability and scars when combined with late gadolinium enhancement (LGE) examination [9–12]. Hence, a combination of myocardial perfusion imaging and CMR-LGE can be used to effectively evaluate the condition of the myocardium; this technique has important diagnostic and prognostic clinical value for patients with AMI.

Resting-state perfusion weight imaging (rs-PWI) refers to perfusion scans conducted directly while the patient is at rest, or in the baseline state. Perfusion image analysis software can obtain the time-myocardium signal curve of the patient, allowing for the calculation of parameters to evaluate myocardial function and microvascular viability [13]. Kiaos et al. previously conducted a meta-analysis of 67 studies (involving 7113 patients with coronary artery disease), and found that, using the fractional flow reserve as a reference standard, the mean sensitivity of perfusion imaging in detecting inadequate blood supply was 90 % (CI: 0.85–0.93) [14]. van Cauteren et al. further demonstrated in their study that combining stress perfusion imaging with rest perfusion imaging and LGE imaging facilitated the accurate diagnosis of coronary artery occlusion in 19 patients with suspected Non-ST segment elevation myocardial infarction (NSTEMI) (overall sensitivity=97 %; specificity=65 %; accuracy=86 %) [15]. Bethke et al. recruited 198 patients with ST-elevation myocardial infarction (STEMI) who underwent rs-PWI, finding that early CMR first-pass perfusion correlated with the prognosis of overall left ventricular function four months after the procedure ($P < 0.001$), indicating its utility in the evaluation of prognostic risk in patients with STEMI [16]. First-pass perfusion at rest has been extensively investigated in the many studies researching AMI; While the technique itself is not new, its application as a resting-first-line imaging tool in acute care settings has not been widely adopted. As such, less is known about the relationship of MVO and parameters of rs-PWI [17–19]. Furthermore, literature on the qualitative and quantitative analysis of rs-PWI, as well as studies on the diagnostic value of MVO, are also limited.

In this context, the present study aimed to explore the clinical application value of rs-PWI sequence of blood perfusion rising slope, perfusion index, peak time, signal intensity and other derived parameters in evaluating MVO in patients with AMI.

2. Methods

2.1. General information

Overall, 566 patients with AMI admitted to the emergency department of a central hospital from September 2016 to August 2024 were reviewed as research objects. The enrollment criteria [20] were as follows: ① Meeting the diagnostic criteria of type I and type II myocardial infarction in the Fourth Edition of Global Unified Definition of Myocardial Infarction (2018); ② Time between symptom onset and admission of $\leq$ 12 hours; ③ PCI was performed and the culprit blood vessels were successfully opened. The exclusion criteria [21] were as follows: ① Missing relevant clinical data; ② Severe valvular heart disease, cardiomyopathy, pregnancy, malignant tumor, severe liver and kidney insufficiency, autoimmune disease, severe infection, pulmonary embolism and other diseases; ③ Cerebrovascular accidents (cerebral hemorrhage, cerebral infarction) in the past six months; ④ History of coronary artery bypass grafting; ⑤ Coronary angiography showing vasospasm and/or myocardial bridge; ⑥ Pregnant or breastfeeding women. Finally, a total of 266 patients were excluded due to lack of relevant clinical data ($n = 142$), other serious diseases ($n = 65$), cerebrovascular accident ($n = 26$), prior history of coronary artery bypass grafting ($n = 15$), coronary angiography suggesting vasospasm, myocardial bridging ($n = 14$), pregnant or breastfeeding women ($n = 4$). The remaining 300 patients were enrolled in the study; this cohort comprised 246 males and 54 females, aged 44–78 years, with a mean age of 58.60 ± 13.03 years, as shown in Fig. 1. All subjects were treated for the first attack of AMI, and CMR examination was performed within 1 week of recanalization.

This study complied with the Helsinki guidelines, and was approved by the ethics committee of XuanWu Hospital. All subjects signed the informed consent form, agreeing to participate.

2.2. Data collection

The following basic data were collected for all patients: Basic data: age, gender, body mass index and heart rate; Cardiac function parameters: end-diastolic volume (EDV), end-systolic volume (ESV), left ventricular ejection fraction (LVEF) and cardiac output (CO); Laboratory test data: myocardial necrosis markers, creatine kinase isoenzyme (CK-MB), troponin (TNI), B-type natriuretic peptide (BNP); Data related to revascularization: thrombolysis in myocardial infarction (TIMI), door to balloon (D2B) time. Finally, the volume of the left ventricle occupied by myocardial infarction (%LV), and the territory vessels were obtained according to the results of digital subtraction angiography (DSA) of coronary arteries.

All imaging data were collected using a Siemens 3.0 T verio scanner (Siemens Magnetom verio 3.0 T), equipped with an 8-channel heart-specific body surface coil. The scanning sequence was as follows: ① T_2WI sequence, TR = 591 ms, TE = 70 ms, TI = 170 ms, flip angle 180 °, FOV = 340 mm × 340 mm, spatial resolution 1.3 mm × 1.3 mm × 6 mm; ② Contrast-enhanced SSFP (CE-SSFP) cine sequence, TR = 3.4 ms, TE = 1.7 ms, flip angle 50 °, FOV = 286 mm × 340 mm, spatial resolution 1.4 mm × 1.8 mm × 8 mm, time resolution 40 ms; ③ For the early gadolinium enhancement (EGE) sequence and late gadolinium enhancement (LGE) sequence, the two acquisition parameters remained consistent, TR = 904 ms, TE = 2 ms, flip angle 20 °, FOV = 360 mm × 360 mm, spatial resolution 1.9 mm × 1.4 mm × 6 mm; ④ rs-PWI sequence, TR = 134 ms, TE = 1.12 ms, TI = 90 ms, flip angle 15 °, FOV = 340 mm × 238 mm, spatial resolution 2.2 mm × 1.8 mm × 6 mm. All sequences were completed in a "one-stop" sequence, with T_2WI, rs-PWI, CE-SSFP cine, EGE (acquisition time 3–5 minutes after contrast injection), LGE (within 15 minutes after contrast injection). T_2WI, CE-SSFP cine, EGE, and LGE sequence scanning positions included two-chamber and four-chamber views, covering 8-slice short-axis images from the bottom of the left ventricular to the apex, while the rs-PWI

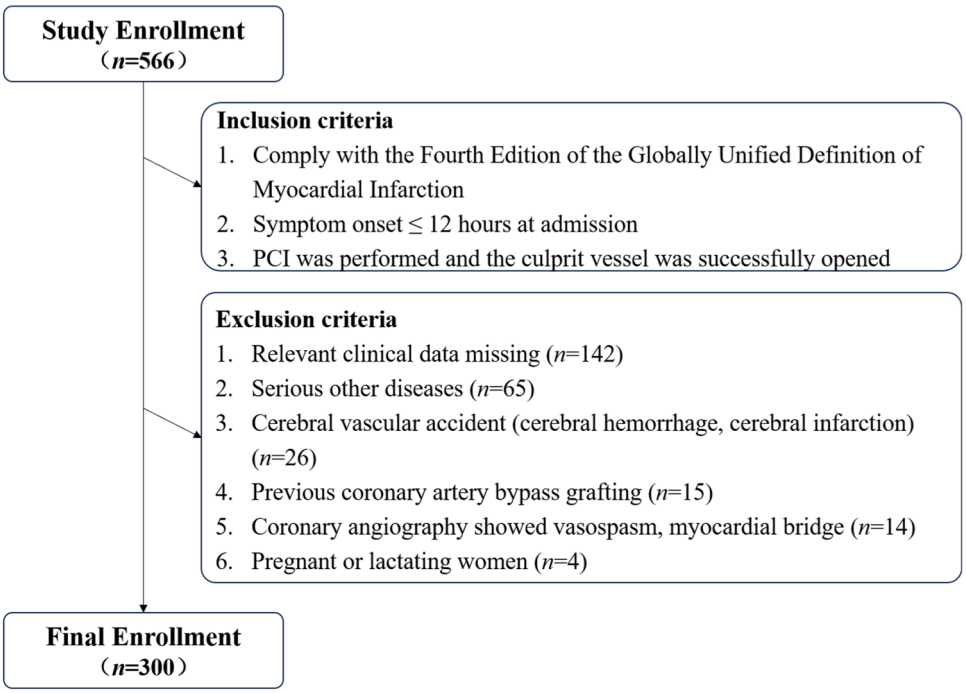

Fig. 1. Patient enrollment flow chart.

sequence includes 1-slice four-chamber view and three-slice short-axis images. The contrast agent was gadopentetate meglumine injection (Beilu Pharmaceutical, National Medicine Approval No. H10860001). The contrast agent was dosed at 0.2 mL/kg, and was injected through the peripheral vein using a high-pressure syringe, at an injection rate of 4.0 mL/s, and the same amount of 0.9 % sodium chloride injection was injected at the same speed.

2.3. Image post processing

All images were analyzed using CVI42 professional cardiac post-processing software (version (5.12. 1) [1688] Circle Cardiovascular Imaging, Calgary, Canada). According to the post-processing standard published by the American Council on Cardiovascular Magnetic Resonance [22], parameters such as EDV, ESV, and LVEF were obtained semi-automatically. According to the classification of American Heart Association [23], the "bull's eye" diagram was used to semi-automatically analyze abnormal wall motion and transmural injury. The left ventricle was divided into 17 segments using the segment division method, while the apical segment that was not conducive to observation and measurement was eliminated, and the corresponding segments under the jurisdiction of the coronary artery supplying blood to the heart were further confirmed. The region of interest (ROI) was semi-automatically delineated on T_2WI and CE-SSFP cine sequences, the remote myocardium at the same level was identified as a reference, and the edematous myocardium based on more than 2 times the standard deviation (SD) was identified [24]. Infarcted myocardium, defined as $>$ 5 SD, was identified on the LGE sequence, and all measurements were taken as a percentage of the left ventricular volume (%LV) [25]. To evaluate the presence of MVO in the infarcted myocardium, the presence of non-enhanced areas in the delayed enhanced myocardium of LGE sequence was taken as the standard, and the segments involved in the "bull's eye" diagram of the myocardium to which MVO belongs were manually labeled [26]. All patients are divided into the MVO positive group ('MVO') or MVO negative group ('non-MVO'), based on the presence of MVO.

2.4. Qualitative evaluation

According to the above classification of the American Heart Association, each patient's myocardium was positioned and segmented again. The myocardium under the territory of the left anterior descending artery (LAD) occupied the 1, 2, 7, 8, 13, and 14 segments, the left circumflex artery (LCX) occupied the 5, 6, 11, 12, and 16 segments, and the right coronary artery (RCA) occupied the 3, 4, 9, 10, and 15 segments. At the segmental level, the degree of delayed myocardial enhancement transmural in patients was classified and recorded. Scores were as follows: no enhancement, 0 points; degree of enhanced transmural penetration 1 %-25 %, 1 point; degree of strengthening penetration of the wall 26 %-50 %, 2 points; degree of strengthening penetration of the wall of 51 %-75 %, 3 points; degree of enhanced transmural penetration of $\geq$ 76 %, 4 points [27]. On the CE-SSFP cine and rs-PWI sequences, the presence or absence of reperfusion myocardial ischemia was judged at the segmental level, while the scores were classified and recorded using a 5-point method, as follows: 0 for none, 1 for suspicious none, 2 for neutral uncertainty, 3 for possible presence of reperfusion myocardial ischemia, and 4 for definite presence [28]. Taking the territory vessels judged by DSA as the "gold standard", the diagnostic sensitivity and specificity of the CE-SSFP cine, EGE and rs-PWI sequences for the level identification of myocardial ischemic segments were obtained [29]. Subsequently, based on the presence or absence of MVO in LGE, the diagnostic value of rs-PWI sequence parameters based on signal intensity curve in myocardial infarction with ischemia-reperfusion and MVO was determined. All of the above evaluations were conducted in a double-blind manner by two doctors with more than 10 years of experience in cardiac magnetic resonance imaging diagnosis. If the opinions were not consistent, the third imaging physician with a senior professional title made the decision.

2.5. Quantitative evaluation

The short-axis first-pass perfusion filling defect and the best level of delayed enhancement clarity were determined on the rs-PWI sequence, and the ROI was sketched in the left ventricular blood pool, with infarcted and remote myocardium both identified. Finally, a time-signal

intensity curve was automatically drawn using software to obtain parameters such as the rising slope, time to peak, signal intensity and myocardial perfusion fraction (MPF), as shown in Fig. 2. The perfusion index was defined as a non-invasive index to quantify myocardial perfusion, reflecting the ratio of the capacity of myocardial capillary bed to the total cardiac volume, using the following calculation formula [27]:

$$MPF = \frac{(\Delta SImyo/\Delta t) - (\Delta SIbase/\Delta t)}{(\Delta SIbp/\Delta t) - (\Delta SIbase/\Delta t)} \quad (1)$$

Where ΔSIrepresents the change in signal intensity, t represents time, subscript "myo" represents myocardium, subscript "bp" represents blood pool, and subscript "base" represents baseline. MPF values are between 0 and 1, normal values are greater than 0.5, and lower MPF values indicate myocardial hypoperfusion.

2.6. Statistical analysis

All statistical analyses were performed using MedCalc software (Version 15.6.1, MedCalc Software bvba, Ostend, Belgium). Normality was determined using the Kolmogorov-Smirnov method. Normally distributed continuous variables are expressed as the mean ± standard deviation, categorical variables are expressed as the frequency or composition ratio (%), and skewed variables are expressed as the median (upper and lower interquartile ranges). Inter-group and within-group comparisons of parameters such as rising slope, peak time, and signal strength were conducted using the analysis of variance or independent, paired sample *t*-test, and multiple comparison corrections were performed. The diagnostic efficacy of CE-SSFP cine, EGE, and rs-PWI sequences for reperfusion myocardial ischemic segments, and the diagnostic efficacy of rs-PWI-derived parameters for MVO were analyzed by construction of receiver operating characteristic (ROC) curves. Statistical significance was set at $P < 0.05$.

3. Results

3.1. Clinical data

The average age of the 300 patients with AMI was 58.60 ± 13.03 years old, and the cohort included 246 males (82 %) and 54 females (18 %). There were 176 patients in the MVO group, with a mean age of 57.90 ± 12.47 years, including 140 males (80 %). There were 124 patients in the non-MVO group, with a mean age of 64.41 ± 8.33 years, including 106 were males (85 %). The laboratory examination of patients in the MVO group revealed the following: CK-MB index 79.16 ± 9.98 IU/L, TNI index 1.80 ± 0.13 ng/mL, and BNP index 401.42 ± 95. 34 pg/mL; values in the non-MVO group were: CK-MB index 70.02 ± 8.75 IU/L, TNI index 1.75 ± 0.20 ng/mL, BNP index 423.67 ± 100.89 pg/mL, with no statistically significant differences ($P > 0.05$).

In the MVO group, patients had mean body mass index 25.13 ± 2.64 kg/m^2, heart rate 66.24 ± 8.63 beats/min, mean end-diastolic volume 110.34 ± 27.98 mL/m^2, end-systolic volume 52.01 ± 15.55 mL/m^2, ejection fraction 43.12 ± 10.76 %, cardiac output 2.99 ± 1.03 L/min; Compared with the non-MVO group, patients had mean body mass index 25.55 ± 3.15 kg/m^2, heart rate 64.60 ± 12.65 beats/min, mean end-diastolic volume 103.25 ± 28.78 mL/m^2, end-systolic volume 60.24 ± 18.86 mL/m^2, ejection fraction 47.11 ± 15.87 %, cardiac output 3.89 ± 1.75 L/min, with no statistically significant differences between the groups ($P > 0.05$).

The territory vessels were determined by coronary angiography in both groups. The MVO group included 135 (76.7 %) cases of grade 3 after thrombolysis in myocardial infarction (TIMI), and the average D2B time of patients was 24.35 ± 7.77 hours. Among the territory vessels, there were 108 (61 %) cases of LAD, 44 (25 %) cases of RCA, and 24 (14 %) cases of LCX. In the non-MVO group, there were 110 (88.7 %) cases of grade 3 after TIMI, and the average D2B time of patients was 28.87 ± 9.92 hours. Among the territory vessels, there were 80 (65 %) cases of LAD, 31 (25 %) cases of RCA, and 13 (10 %) cases of LCX

The left ventricular volumes occupied by the infarcted myocardium were 19.60 ± 2.70 %LV and 15.20 ± 3.40 %LV in the MVO and non-MVO groups, respectively, yielding a statistically significant difference ($P < 0.05$). For more details see Table 1.

3.2. Qualitative diagnostic value of rs-PWI

Among the 300 patients with AMI, a total of 4800 segments were included in the statistical analysis, of which 1509 myocardial segments showed LGE.

The first-pass ROC curve analysis of CE-SSFP cine, EGE, and rs-PWI for AMI as a whole showed that the highest area under curve (AUC) of rs-PWI was 0.93 (0.91–0.96), the sensitivity was 92.4 %, the specificity was 92.6 %, and the Youden index was 0.85. In the MVO group, the AUC of rs-PWI was 0.95 (0.89–0.99), the sensitivity was 94.3 %, the specificity was 93.4 %, and the Youden index was 0.88. Compared with the ROC curves of rs-PWI and EGE sequences on reperfusion myocardial

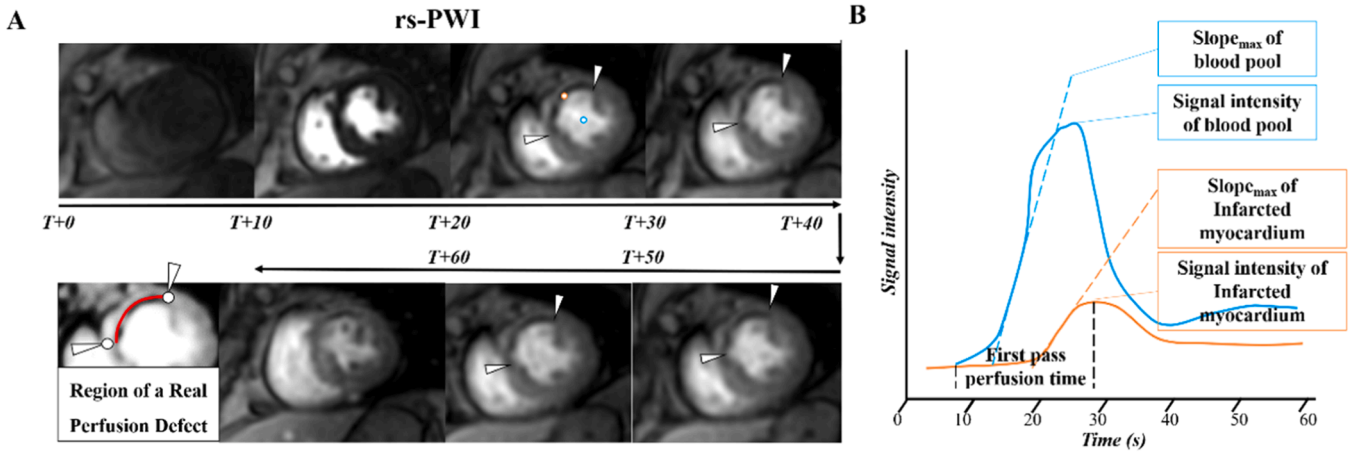

Fig. 2. Schematic diagram of the time-signal intensity curve of the left ventricular blood pool and infarcted myocardium in resting-state perfusion imaging (rs-PWI). 2 A) A 72-year-old male patient underwent CMR examination after percutaneous coronary intervention (PCI). Resting-state perfusion imaging (rs-PWI) revealed transmural infarction of the anterior septal wall with microvascular obstruction (indicated by the white arrow). The region of interest was outlined in the left ventricular blood pool (blue circle) and infarcted myocardium (orange circle) at the level with the clearest short-axis perfusion filling defect and delayed enhancement; 2B) The time-signal intensity curve was automatically drawn to obtain parameters such as the rising slope, time to peak and signal intensity.

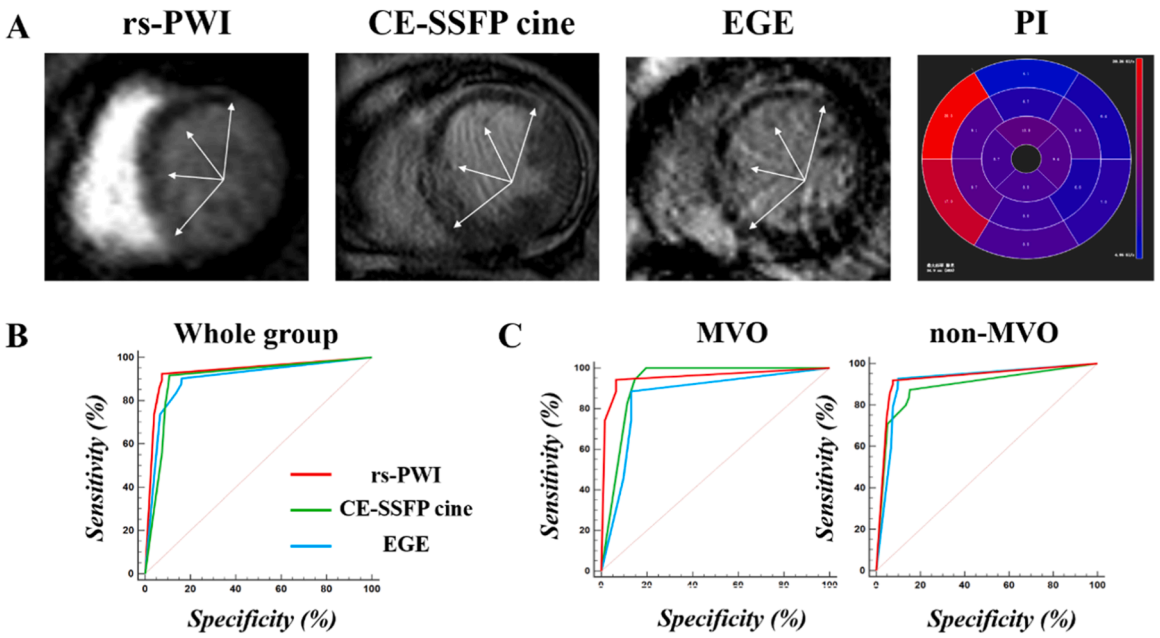

Fig. 3. *Diagnostic value of rs-PWI for myocardial ischemia.* 3 A) CMR rs-PWI, CE-SSFP cine, EGE, and segmental perfusion index bull's eye analysis showed myocardial ischemia, and the range of filling defect was shown by the white arrow; 3B) The diagnostic efficacy of rs-PWI, CE-SSFP cine, and EGE for reperfused myocardial ischemia in the whole group patients included; 3 C) The diagnostic efficacy for reperfused myocardial ischemia in the MVO group and the non-MVO group.

Table 1
Characteristics of Acute MI patients.

Characteristics		Whole Groups ($n = 300$)	MVO ($n = 176$)	non-MVO ($n = 124$)	*F*-value	*P*-value
Age (yrs)		58.60 ± 13.03	57.90 ± 12.47	64.41 ± 8.33	2.699	0.069
Male (Male gender %)		246 (82)	140 (80)	106 (85)	1.359	0.067
BMI (kg/m^2)		25.20 ± 2.72	25.13 ± 2.64	25.55 ± 3.15	0.209	0.812
Heart rate (beat/min)		65.98 ± 9.35	66.24 ± 8.63	64.60 ± 12.65	0.258	0.773
Cardiac function						
EDV/BSA (mL/m^2)		108.43 ± 35.59	110.34 ± 27.98	103.25 ± 28.78	0.304	0.686
ESV/BSA (mL/m^2)		56.97 ± 19.06	52.01 ± 15.55	60.24 ± 18.86	0.244	0.670
LVEF (%)		46.85 ± 12.69	43.12 ± 10.76	47.11 ± 15.87	0.397	0.509
CO (L/min)		3.78 ± 1.36	2.99 ± 1.03	3.89 ± 1.75	3.011	0.102
Laboratory	CK-MB (IU/L)	72.17 ± 10.46	79.16 ± 9.98	70.02 ± 8.75	2.780	0.070
	TNI (ng/mL)	1.76 ± 0.16	1.80 ± 0.13	1.75 ± 0.20	0.333	0.781
	BNP (pg/mL)	422.21 ± 121.14	401.42 ± 95.34	423.67 ± 100.89	1.798	0.145
Revascularization	TIMI flow post-PCI (%)	245 (81.6)	135 (76.7)	110 (88.7)	6.224	0.143
	Door to balloon time (h)	28.58 ± 8.31	24.35 ± 7.77	28.87 ± 9.92	0.205	0.668
Infarcted myocardial volume (%LV)		17.90 ± 2.80	19.60 ± 2.70	15.20 ± 3.40	2.987	**< 0.05**
Culprit vessel by angiography						
LAD (%)		188 (63)	108 (61)	80 (65)	-	-
LCX (%)		37 (12)	24 (14)	13 (10)	-	-
RCA (%)		75 (25)	44 (25)	31 (25)	-	-

-Note: AMI: acute myocardial infarction; BSA: body mass index; MVO: microvascular obstruction; LAD: left anterior descending artery; LCX: left circumflex artery; PCI: percutaneous coronary intervention; RCA: right coronary artery; TIMI: thrombolysis in myocardial infarction. Values are mean ± SD or n (%).

ischemia at the segmental level, the difference was statistically significant ($P < 0.05$). In the non-MVO group, the AUC of rs-PWI was 0.93 (0.89–0.95), the sensitivity was 91.8 %, the specificity was 92.4 %, and the Youden index was 0.84. The difference between the ROC curves of rs-PWI and the CE-SSFP cine sequence on reperfusion myocardial ischemia at the segmental level was statistically significant ($P < 0.05$), as shown in Table 2.

3.3. Comparison of semi-quantitative parameters of segmental level rs-PWI

The maximum rising slope of the MVO group was statistically significantly higher than that of the non-MVO group (15.09 ± 2.64 vs. 6.21 ± 1.25, $t = -3.482$, $P < 0.05$). The peak time of 20 %-80 % of patients in the MVO group was significantly shorter than that in the non-MVO group (4.07 ± 0.79 vs. 7.75 ± 1.03, $t = 4.243$, $P < 0.05$). The differences between the two groups in the baseline ratio of maximum rising slope, perfusion index, maximum signal intensity, and baseline ratio of maximum signal intensity were also statistically significant ($P < 0.05$), as shown in Table 3.

3.4. Diagnostic value of semi-quantitative parameters of rs-PWI

ROC curve analysis further revealed that the diagnostic AUC of perfusion index, maximum signal intensity, peak to time (20 %-80 %) and maximum rising slope for MVO in CMR myocardial perfusion imaging parameters were 0.90, 0.88, 0.85 and 0.75, respectively, while the sensitivity, specificity and accuracy of perfusion index were 94.1 %,

Table 2
Qualitative diagnostic value of rs-PWI in reperfusion myocardial ischemia.

	Sensitivity (%)	Specificity (%)	Youden index	AUC [95 % CI]	*P*-value
Whole Groups (*n* = *4800*)					
CE-SSFP cine	90.3 [84.3–94.6]	83.8 [78.8–87.9]	0.74	0.90 [0.87–0.93]	cine vs. EGE: 0.86
EGE	91.7 [86.0–95.7]	89.3 [85.0–92.7]	0.81	0.90 [0.87–0.93]	**cine vs. rs-PWI: < 0.05**
rs-PWI	92.4 [86.8–96.2]	92.6 [88.8–95.4]	0.85	0.93 [0.91–0.96]	EGE vs. rs-PWI: 0.10
MVO (*n* = *2816*)					
CE-SSFP cine	100.0 [90.0–100.0]	80.3 [68.2–89.4]	0.80	0.93 [0.86–0.97]	cine vs. EGE: 0.11
EGE	88.6 [73.3–96.8]	86.9 [75.8–94.2]	0.75	0.86 [0.78–0.92]	cine vs. rs-PWI: 0.36
rs-PWI	94.3 [80.8–99.3]	93.4 [84.1–98.2]	0.88	0.95 [0.89–0.99]	**EGE vs. rs-PWI: < 0.05**
non-MVO (*n* = *1984*)					
CE-SSFP cine	87.3 [79.6–92.9]	84.8 [79.2–89.3]	0.72	0.89 [0.85–0.92]	cine vs. EGE: 0.16
EGE	92.7 [86.2–96.8]	90.0 [85.1–93.7]	0.83	0.91 [0.88–0.94]	**cine vs. rs-PWI: < 0.05**
rs-PWI	91.8 [85.0–96.2]	92.4 [87.9–95.6]	0.84	0.93 [0.89–0.95]	EGE vs. rs-PWI: 0.51

-Note：CE-SSFP cine: contrast-enhanced SSFP cine; EGE: early gadolinium enhancement; rs-PWI: resting-state perfusion weighted imaging; AUC: area under curve.

Table 3
Comparison of segmental level rs-PWI imaging parameters between MVO group and non-MVO group.

	MVO (*n* = *679*)	non-MVO (*n* = *830*)	*t*-value	*P*-value
$Slope_{max}$	15.09 ± 2.64	6.21 ± 1.25	−3.482	**< 0.05**
$Slope_{max}$ of baseline (%)	202.84 ± 37.09	85.52 ± 13.99	−3.675	**< 0.05**
PI	0.32 ± 0.09	0.42 ± 0.04	2.404	**< 0.05**
T_{Max} (s)	17.64 ± 0.19	25.66 ± 3.08	1.722	0.107
$T_{50\ \%\ of\ Max}$ (s)	15.51 ± 0.44	21.01 ± 2.42	1.496	0.156
$T_{20–80\ \%\ of\ Max}$ (s)	4.07 ± 0.79	7.75 ± 1.03	4.243	**< 0.05**
SI_{max}	74.51 ± 8.05	35.09 ± 5.51	−4.018	**< 0.05**
SI_{max} of baseline (%)	1000.54 ± 117.85	488.06 ± 62.15	−4.241	**< 0.05**
$SI_{baseline}$	7.48 ± 0.17	7.02 ± 0.26	−1.119	0.282

-Note: PI: perfusion index; SI: signal intensity; T: time to peak. Values are mean ± SD.

88.7 % and 91.1 %.

4. Discussion

The rs-PWI plays a central role in the diagnosis, management, and risk stratification of patients with AMI, providing rich information regarding coronary microvascular function; as such, it is recommended by the international guidelines [30]. Therefore, based on the time series acquisition of rs-PWI, this study sensitively captured the dynamic filling process of the left ventricular cavity after the first perfusion of contrast agent, and effectively judged reperfusion myocardial ischemia by observing whether there is a decreased area of myocardial perfusion, combined with gadolinium enhancement sequence, so as to realize the image-assisted evaluation of AMI patients with MVO.

Myocardial infarction has been described as extending from the endocardium to the epicardium in the form of a "waterfront" [31]; however, recent studies have found that infarction can also cause myocardial necrosis due to the destruction of the microvascular network downstream of epicardial coronary arteries [26]. This suggests that vascular injury in reperfusion AMI may be the cause of secondary myocardial necrosis and MVO. Therefore, the unique feature of the rs-PWI sequence is that it uses the positive correlation between contrast agent concentration and CMR scanning signal intensity to both indirectly and semi-quantitatively reflect the influence range of MVO on myocardium by measuring the time-signal intensity curve in the region of interest [32]. Firstly, we took the segment of the territory vessels of DSA as the "gold standard", finding that rs-PWI can not only sensitively reflect the location of myocardial ischemia in patients with AMI, but also maintain consistency with EGE and CE-SSFP cine, with a high diagnostic sensitivity and specificity. At the segmental level of the MVO group, the sensitivity of rs-PWI at identifying MVO reached 94.3 %, with a specificity of 93.4 %, and an AUC of 0.95. Prior research has shown that the identification of MVO can effectively compensate for the false negative judgment at the junction of LGE "black blood" blood pool and endocardial MVO through CE-SSFP cine, which is due to the "bright blood" of cine and the low signal of MVO in infarcted myocardium, forming a signal contrast of "white-black-white" from endocardium to epicardium. Matsumoto et al. previously showed that the subendocardial infarction signal changes dynamically within a short time of contrast injection [33]. Therefore, in the CMR scanning process, rs-PWI uses multiple cardiac cycles, realizing a dynamic acquisition process from the beginning of contrast medium injection to the end of first-pass perfusion, which is more conducive to the immediate judgment and detection of MVO at the level of segments by images.

In the present study, the maximum rising slope and time to the peak of the rs-PWI sequence derived parameters were measured to reflect the myocardial perfusion velocity and perfusion degree, while myocardial perfusion was comprehensively evaluated from the segmental level. Our analysis showed that the maximum rising slope of MVO group was higher than that of non-MVO group, and the peak time of the first perfusion was decreased by 20 %-80 %, indicating the existence of a decrease in blood flow in MVO area, causing a large influx of contrast agent into the reperfused myocardium outside MVO. Under the premise that the epicardial vessels have been opened, because the diameter of the anterior arterioles is only 100–500 microns (while the diameter of the tiny vessels is less than 100 microns), MVO is still an important reason for the phenomenon of "no reflow" of myocardial blood flow [34]. As such, it is the stenosis or even occlusion of vascular lumen caused by MVO that leads to reperfusion myocardial injury, and even intramyocardial hemorrhage. Analyzing the reasons from a technical perspective, the following points must be considered: 1) Selection of ROI: In this paper, the infarcted myocardium area and blood pool area were taken for post-processing calculation (as shown in Fig. 2). The infarcted area contains the infarcted core and MVO; the contrast agent can be quickly cleared in normal myocardium, but the contrast agent retains in the infarcted myocardium, and MVO forms a protective layer similar to an "amber", making it difficult for the contrast agent to enter. The uncertainty of ROI selection means that the rising slope and peak time of perfusion could have been underestimated. 2) The rs-PWI is a continuous dynamic acquisition of T1-weighted images based on planar echoes, and the first-pass perfusion of contrast agent is measured to contrast with the plain scan, while the acquired R-R interval is related to the heart rate. The rs-PWI is acquired as a timing sequence over several consecutive cardiac cycles. In the present study, the basal heart rate of patients in the MVO group was faster than that in the non-MVO group (MVO: 66.24 ± 8.63 beats/min vs. non-MVO: 64.60 ± 12.65 beats/min). Although the difference did not reach statistical significance, in the first several R-R intervals of rs-PWI collection, heart rate was an important factor affecting the postprocessing curve, while the shortening of the R-R interval led to an increase in the curve slope. 3) The MVO or accompanied by intramyocardial hemorrhage [26]. The

Canadian Cardiovascular Society's new classification consensus for AMI, was set based on the severity of myocardial injury points out that grade IV is myocardial necrosis and microvascular necrosis leading to reperfusion bleeding. Patients in the MVO group included in this study were not screened by sequences such as T2 * mapping. When the contrast agent enters the myocardium, the change in the myocardial signal intensity depends on the tissue perfusion, blood flow, extracellular space, and the distribution of the contrast agent in the myocardium. If there is a tiny blood vessel rupture, the peak time of myocardial bleeding is bound to be shortened by segmental level blood perfusion.

It is also worth mentioning that the perfusion index (MFF) was at the segmental level (MVO: 0.32 ± 0.09 vs. non-MVO: 0.42 ± 0.04), and the difference between the two groups was statistically significant. Further ROC curve analysis revealed that the highest diagnostic value of perfusion index for MVO was AUC 0.90 (0.84–0.97), with a sensitivity of 94.1 %, specificity of 88.7 %, and accuracy of 91.1 %. The segmental level MFF decreased to 0.3, which also indicated that myocardial blood perfusion could not be basically guaranteed due to the existence of MVO. Combined with the above findings, the authors speculate that rs-PWI has the potential to quantify myocardial blood flow; however, further research is required to determine the best model, and the perfusion parameters of semi-quantitative CMR need to be standardized and verified before it can be safely implemented in clinical practice.

4.1. Limitations

This study has several limitations. (1): This study followed a single-center design, and the rs-PWI sequences were based on the Siemens 3.0 T verio model. Temporal resolution and high signal-to-noise ratio remain critical needs to ensure imaging quality. Whether the derived parameters are extensive and applicable requires further multi-center and multi-model research. (2) Considering the condition of patients with AMI, particularly those with MVO, symptoms are often severe. As an important part of the CMR scanning module, rs-PWI lasts for a long time, which some patients are unable to tolerate, eventually leading to scan failure. (3) Further, the calculation method for the time-signal curve of the derived parameters can be further optimized, and the influence of confounding factors could be eliminated through implementation of multi-factor analysis. The conclusions obtained still need to be confirmed by subsequent larger multi-center prospective studies. (4) Finally, the CMR scanning process is complicated, and requires experienced technicians to operate, which further limits the scope of application.

5. Conclusion

Overall, the results of this study showed that cardiac magnetic resonance rs-PWI sequence can effectively qualitatively evaluate reperfusion myocardial ischemia, semi-quantitatively evaluate the influence range and degree of microcirculation obstruction, and perfusion index has high diagnostic value for qualitative identification of MVO.

Ethical statement

This study complied with the Helsinki guidelines, and was approved by the ethics committee of XuanWu Hospital. All subjects signed the informed consent form, agreeing to participate.

Funding

This study was supported by National Natural Science Foundation of China (62172288); Capital Medical University Undergraduate Innovation Project (XSKY2024396); Xuanwu Hospital of Capital Medical University Clinical Research Project (LCYJ202410).

CRediT authorship contribution statement

Zhi Liu: Supervision, Resources, Project administration. **Wang ZiDi:** Writing – original draft, Investigation, Data curation. **Hu YingYing:** Writing – original draft, Methodology. **Jie Lu:** Writing – review & editing, Supervision. **Zheng Sun:** Writing – review & editing, Project administration.

Declaration of Generative AI and AI-assisted technologies in the writing process

The authors declare that they do not use any AI tools in scientific writing in this paper.

Declaration of Competing Interest

The authors declare that they have no known competing financial interests or personal relationships that could have appeared to influence the work reported in this paper.

Data availability

Data will be made available on request.

References

[1] J.E. Tamis-Holland, J.D. Abbott, K. Al-Azizi, N. Barman, A.E. Bortnick, M.G. Cohen, P. Dehghani, T.D. Henry, F. Latif, M. Madjid, C.M. Yong, Y. Sandoval, SCAI expert consensus statement on the management of patients with STEMI referred for primary PCI, J. Soc. Cardiovasc Angiogr. Inter. 3 (2024) 102294 https://doi.10.1016/j.jscai.2024.

[2] S. Limalanathan, G.Ø. Andersen, N. Kløw, M. Abdelnoor, P. Hoffmann, J. Eritsland, Effect of ischemic postconditioning on infarct size in patients with ST-elevation myocardial infarction treated by primary PCI results of the POSTEMI (POstconditioning in ST-Elevation Myocardial Infarction) randomized trial, JAHA 3 (2014) 679, https://doi.org/10.1161/jaha.113.000679.

[3] S.T. Hussain, M. Paul, S. Plein, G.P. McCann, A.M. Shah, M.S. Marber, A. Chiribiri, G. Morton, S. Redwood, P. MacCarthy, A. Schuster, M. Ishida, M.A. Westwood, D. Perera, E. Nagel, Design and rationale of the MR-INFORM study: stress perfusion cardiovascular magnetic resonance imaging to guide the management of patients with stable coronary artery disease, J. Cardiovasc Magn. Reson 14 (2012) 65, https://doi.10.1186/1532-429X-14-65.

[4] C. Shetelig, S. Limalanathan, J. Eritsland, P. Hoffmann, I. Seljeflot, J.M. Gran, P. Aukrust, T. Ueland, G.Ø. Andersen, Osteoprotegerin levels in ST-elevation myocardial infarction: Temporal profile and association with myocardial injury and left ventricular function, Plos ONE 12 (2017) e0173034, https://doi.org/10.1371/journal.pone.0173034.

[5] A. Bethke, L. Shanmuganathan, G.Ø. Andersen, J. Eritsland, D. Swanson, N. E. Kløw, P. Hoffmann, Microvascular perfusion in infarcted and remote myocardium after successful primary PCI: angiographic and CMR findings, Eur. Radio. 29 (2019) 941–950, https://doi.org/10.1007/s00330-018-5588-7.

[6] X. Wang, J. Pu, Recent advances in cardiac magnetic resonance for imaging of acute myocardial infarction (Small Methods 3/2024), Small Methods 8 (2024) 2301170, https://doi.org/10.1002/smtd.202470014.

[7] V.O. Puntmann, S. Valbuena, R. Hinojar, S.E. Petersen, J.P. Greenwood, C. M. Kramer, R.Y. Kwong, G.P. McCann, C. Berry, E. Nagel, C. Berry, D. Bluemke, J. Bremerich, R. Botnar, C. Bucciarelli-Ducci, R.P. Choudhury, M. Dweck, I. Eitel, V. Ferrari, M. Friedrich, J. Greenwood, R. Hinojar, G. Hundley, C.M. Kramer, R. Y. Kwong, M. Lombardi, T. Lopez Fernandez, T. Marwick, E. Nagel, J. Narula, S. Neubauer, A. Patel, D. Pennell, S.E. Petersen, S. Plein, S. Prasad, V.O. Puntmann, F. Rademakers, S. Raman, H. Sakuma, J. Sanz, J. Schulz-Menger, O. Simonetti, A. Swift, A.J. Taylor, T. Teixeira, H. Thiele, M. Ugander, S. Valbuena, J. J. Westenberg, A.A. Young, Society for Cardiovascular Magnetic Resonance (SCMR) expert consensus for CMR imaging endpoints in clinical research: part I - analytical validation and clinical qualification, J. Cardiovasc. Magn. R. 20 (2018) 67, https://doi.org/10.1186/s12968-018-0484-5.

[8] M.G. Del Buono, R.A. Montone, M. Camilli, S. Carbone, J. Narula, C.J. Lavie, G. Niccoli, F. Crea, Coronary microvascular dysfunction across the spectrum of cardiovascular diseases, J. Am. Coll. Cardiol. 78 (2021) 1352–1371, https://doi.org/10.1016/j.jacc.2021.07.042.

[9] J.P. Greenwood, N. Maredia, J.F. Younger, J.M. Brown, J. Nixon, C.C. Everett, P. Bijsterveld, J.P. Ridgway, A. Radjenovic, C.J. Dickinson, S.G. Ball, S. Plein, Cardiovascular magnetic resonance and single-photon emission computed tomography for diagnosis of coronary heart disease (CE-MARC): a prospective trial, Lancet 379 (2012) 453–460, http://doi.10.1016/S0140-6736(11)61335-4.

[10] M. Deschner, A. Glanz, Magnetic resonance perfusion or fractional flow reserve in coronary disease, N. Engl. J. Med. 381 (2019) 2276–2278, https://doi.org/10.1056/nejmc1913968.

[11] M. Li, T. Zhou, L.F. Yang, Z.H. Peng, J. Ding, G. Sun, Diagnostic accuracy of myocardial magnetic resonance perfusion to diagnose ischemic stenosis with fractional flow reserve as reference, Syst. Rev. meta-Anal. JACC Cardiovasc Imaging 7 (2014) 1098–1105, https://doi.org/10.1016/j.jcmg.2014.07.011.
[12] O.R. Coelho-Filho, C. Rickers, R.Y. Kwong, M. Jerosch-Herold, MR myocardial perfusion imaging, Radiology 266 (2013) 701–715, https://doi.org/10.1148/radiol.12110918.
[13] X.-M. Li, L. Jiang, C.-Y. Min, W.-F. Yan, M.-T. Shen, X.-J. Liu, Y.-K. Guo, Z.-G. Yang, Myocardial perfusion imaging by cardiovascular magnetic resonance: Research progress and current implementation, Curr. Probl. Cardiol. 48 (2023) 101665, https://doi.org/10.1016/j.cpcardiol.2023.101665.
[14] A. Kiaos, I. Tziatzios, S. Hadjimiltiades, C. Karvounis, T.D. Karamitsos, Diagnostic performance of stress perfusion cardiac magnetic resonance for the detection of coronary artery disease, Int. J. Cardiol. 252 (2018) 229–233, https://doi.org/10.1016/j.ijcard.2017.11.066.
[15] Y.J.M. van Cauteren, M.W. Smulders, R.A.L.J. Theunissen, S.C. Gerretsen, B. P. Adriaans, G.P. Bijvoet, A.M.A. Mingels, S.M.J. van Kuijk, S. Schalla, H.J.G. M. Crijns, R.J. Kim, J.E. Wildberger, J. Heijman, S.C.A.M. Bekkers, Cardiovascular magnetic resonance accurately detects obstructive coronary artery disease in suspected non-ST elevation myocardial infarction: a sub-analysis of the CARMENTA Trial, J. Cardiovasc. Magn. R. 23 (2021) 40, https://doi.org/10.1186/s12968-021-00723-6.
[16] A. Bethke, L. Shanmuganathan, G.Ø. Andersen, J. Eritsland, D. Swanson, N. E. Kløw, P. Hoffmann, Microvascular perfusion in infarcted and remote myocardium after successful primary PCI: angiographic and CMR findings, Eur. Radio. 29 (2019) 941–950, https://doi.org/10.1007/s00330-018-5588-7.
[17] A. Mayr, K. Pedarnig, G. Klug, M. Schocke, O. Pachinger, W. Jaschke, B. Metzler, Regional functional recovery after acute myocardial infarction: A cardiac magnetic resonance long-term study, Int J. Cardiovasc Imaging 28 (2012) 1445–1453, https://doi.org/10.1007/s10554-011-9951-x.
[18] T. Baks, R.-J. van Geuns, E. Biagini, P. Wielopolski, N.R. Mollet, F. Cademartiri, E. Boersma, W.J. van der Giessen, G.P. Krestin, D.J. Duncker, P.W. Serruys, P.J. de Feyter, Recovery of left ventricular function after primary angioplasty for acute myocardial infarction, Eur. Heart J. 26 (2005) 1070–1077, https://doi.org/10.1093/eurheartj/ehi131.
[19] J. Schwitter, C.M. Wacker, A.C. van Rossum, M. Lombardi, N. Al-Saadi, H. Ahlstrom, T. Dill, H.B. Larsson, S.D. Flamm, M. Marquardt, L. Johansson, MR-IMPACT: comparison of perfusion-cardiac magnetic resonance with single-photon emission computed tomography for the detection of coronary artery disease in a multicentre, multivendor, randomized trial, Eur. Heart J. 29 (2008) 480–489, http://doi.10.1093/eurheartj/ehm617.
[20] J.S. Thygesen, A.S. Alpert, B. Jaffe, J.J.R. Chaitman, D.A. Bax, H.D. Morrow, White, Executive Group on behalf of the Joint European Society of Cardiology (ESC)/American College of Cardiology (ACC)/American Heart Association (AHA)/World Heart Federation (WHF) Task Force for the Universal Definition of Myocardial Infarction. Fourth Universal Definition of Myocardial Infarction, J. Am. Coll. Cardiol. 72 (2018) (2018) 2231–2264, https://doi.org/10.1016/j.jacc.2018.08.1038.
[21] A.R. Payne, M. Casey, J. McClure, R. McGeoch, A. Murphy, R. Woodward, A. Saul, X. Bi, S. Zuehlsdorff, K.G. Oldroyd, N. Tzemos, C. Berry, Bright-blood T2-weighted MRI has higher diagnostic accuracy than dark-blood short tau inversion recovery MRI for detection of acute myocardial infarction and for assessment of the ischemic area at risk and myocardial salvage, Circ. Cardiovasc Imaging 4 (2011) 210–219, https://doi.org/10.1161/circimaging.110.960450.
[22] J. Schulz-Menger, D.A. Bluemke, J. Bremerich, S.D. Flamm, M.A. Fogel, M. G. Friedrich, R.J. Kim, F. von Knobelsdorff-Brenkenhoff, C.M. Kramer, D.J. Pennell, S. Plein, E. Nagel, Standardized image interpretation and post processing in cardiovascular magnetic resonance - 2020 update: Society for Cardiovascular Magnetic Resonance (SCMR): Board of Trustees Task Force on Standardized Post Processing, J. Cardiovasc. Magn. R. 22 (2020) 19, https://doi.org/10.1186/1532-429x-15-35.
[23] W.G. Hundley, D.A. Bluemke, J.P. Finn, S.D. Flamm, M.A. Fogel, M.G. Friedrich, V. B. Ho, M. Jerosch-Herold, C.M. Kramer, W.J. Manning, M. Patel, G.M. Pohost, A. E. Stillman, R.D. White, P.K. Woodard, expert consensus document on cardiovascular magnetic resonance: A report of the American College of Cardiology Foundation Task Force on Expert Consensus Documents, Circulation 121 (2010) 2462–2508, https://doi.org/10.1161/CIR.0.
[24] C. Göransson, K.A. Ahtarovski, K. Kyhl, J. Lønborg, L. Nepper-Christensen, L. Bertelsen, A.A. Ghotbi, M.M. Schoos, L. Køber, D. Høfsten, S. Helqvist, H. Kelbæk, T. Engstrøm, N. Vejlstrup, Assessment of the myocardial area at risk: comparing T2-weighted cardiovascular magnetic resonance imaging with contrast-enhanced cine (CE-SSFP) imaging—a DANAMI3 substudy, Eur. Heart J. Cardiovasc Imaging 20 (2019) 361–366, https://doi.org/10.1093/ehjci/jey106.
[25] E. Heiberg, M. Ugander, H. Engblom, M. Götberg, G.K. Olivecrona, D. Erlinge, H. Arheden, Automated quantification of myocardial infarction from MR images by accounting for partial volume effects: animal, phantom, and human study, Radiology 246 (2008) 581–588, https://doi.org/10.1148/radiol.2461062164.
[26] K.P. Vora, A. Kumar, M.S. Krishnam, F.S. Prato, S.V. Raman, R. Dharmakumar, Microvascular obstruction and intramyocardial hemorrhage in reperfused myocardial infarctions, Pathophysiol. Clin. Insights Imaging JACC Cardiovasc Imaging 17 (2024) 795–810, https://doi.org/10.1016/j.jcmg.2024.02.003.
[27] A. Seraphim, K.D. Knott, A.-M. Beirne, J.B. Augusto, K. Menacho, J. Artico, G. Joy, R. Hughes, A.N. Bhuva, R. Torii, H. Xue, T.A. Treibel, R. Davies, J.C. Moon, D. A. Jones, P. Kellman, C. Manisty, Use of quantitative cardiovascular magnetic resonance myocardial perfusion mapping for characterization of ischemia in patients with left internal mammary coronary artery bypass grafts, J. Cardiovasc. Magn. R. 23 (2021) 82, https://doi.org/10.1186/s12968-021-00763-y.
[28] C. Kim, C.H. Park, D.Y. Kim, J. Cha, B.Y. Lee, C.H. Park, E.-J. Kang, H.J. Koo, K. Kitagawa, M.J. Cha, R. Krittayaphong, S.I. Choi, S. Viswamitra, S.M. Ko, S. M. Kim, S.H. Hwang, N.N. Trang, W. Lee, Y.J. Kim, J. Lee, D.H. Yang, Semi-quantitative scoring of late gadolinium enhancement of the left ventricle in patients with ischemic cardiomyopathy: Improving interobserver reliability and agreement using consensus guidance from the Asian Society of Cardiovascular Imaging-Practical Tutorial (ASCI-PT) 2020, Korean J. Radio. 23 (2022) 298, https://doi.org/10.3348/kjr.2021.0387.
[29] H. Arheden, Myocardium at risk by early gadolinium enhancement MR imaging, A Mov. Target? JACC Cardiovasc Imaging 10 (2017) 140–142, https://doi.org/10.1016/j.jcmg.2016.03.020.
[30] J. Knuuti, W. Wijns, A. Saraste, D. Capodanno, E. Barbato, C. Funck-Brentano, E. Prescott, R.F. Storey, C. Deaton, T. Cuisset, S. Agewall, K. Dickstein, T. Edvardsen, J. Escaned, B.J. Gersh, P. Svitil, M. Gilard, D. Hasdai, R. Hatala, F. Mahfoud, J. Masip, C. Muneretto, M. Valgimigli, S. Achenbach, J.J. Bax, ESC Scientific Document Group. 2019, ESC Guidelines for the diagnosis and management of chronic coronary syndromes, Eur. Heart J. 41 (2019) 407–477, https://doi.org/10.1093/eurheartj/ehz425.
[31] O. Sorop, J. van de Wouw, S. Chandler, V. Ohanyan, J.D. Tune, W.M. Chilian, D. Merkus, S.B. Bender, D.J. Duncker, Experimental animal models of coronary microvascular dysfunction, Cardiovasc. Res. 116 (2020) 756–770, https://doi.org/10.1093/cvr/cvaa002.
[32] A.R. Patel, M. Salerno, R.Y. Kwong, A. Singh, B. Heydari, C.M. Kramer, Stress cardiac magnetic resonance myocardial perfusion imaging: JACC review topic of the week, J. Am. Coll. Cardiol. 78 (2021) 1655–1668, https://doi.org/10.1016/j.jacc.2021.08.022.
[33] H. Matsumoto, T. Matsuda, K. Miyamoto, T. Shimada, S. Ushimaru, M. Mikuri, T. Yamazaki, Temporal change of enhancement after gadolinium injection on contrast-enhanced CMR in reperfused acute myocardial infarction, J. Cardiol. 65 (2015) 76–81, https://doi.org/10.1016/j.jjcc.2014.04.005.
[34] D.J. Doherty, R. Sykes, K. Mangion, C. Berry, Predictors of microvascular reperfusion after myocardial infarction, Curr. Cardiol. Rep. 23 (2021) 21, https://doi.org/10.1007/s11886-021-01442-1.